Aquatic Sciences (2026) 88:68
https://doi.org/10.1007/s00027-026-01299-y

Aquatic Sciences

RESEARCH ARTICLE

Planktonic response to pulse or continuous inorganic nutrient inputs: temporal variations and monitoring implications

Warren Meredith[1] · Nuria Perujo[2,3] · María Antón-Pardo[3,4] · Anna M. Romaní[3] · Dani Boix[3] · Jordi Compte[3] · María Bas-Silvestre[3] · Xavier D. Quintana[3] · Anna Menció[5]

Received: 13 October 2025 / Accepted: 23 March 2026 / Published online: 8 April 2026

Abstract

Coastal lagoons are dynamic systems where the mode of nutrient input, continuous or pulsed, or a combination, can significantly affect plankton community structure and function. We conducted a spring field microcosm experiment in a Mediterranean lagoon to evaluate how three nutrient delivery regimes influence planktonic dynamics, using biomass measurements and extracellular enzyme activity (EEA) as functional indicators. Continuous nutrient additions promoted sustained phytoplankton and bacterioplankton growth, indicating bottom-up control and microbial stability. In contrast, pulse treatments saw a brief bacterioplankton bloom followed by delayed phytoplankton increase and a marked decline in zooplankton, suggesting disrupted trophic succession and food quality limitations. The pulse–continuous treatment yielded intermediate responses, confirming that delivery mode, not just nutrient load, modulates ecosystem processes. Elevated β-glucosidase (GLU) and leucine aminopeptidase (LAP) activity under nutrient addition, particularly in continuous treatments, signaled intensified carbon and nitrogen demand and active organic matter mineralization, even when nutrient concentrations appeared low. These findings suggest that, during stable spring conditions, microbial communities rapidly assimilate nutrients, potentially obscuring short-term biogeochemical changes from traditional concentration-based monitoring. Crucially, the timing and frequency of nutrient supply are as influential as total input, with continuous inputs supporting a more stable and efficient microbial loop. This work underscores the ecological importance of recognizing diffuse, low-level nutrient sources, such as groundwater seepage, which may be underrepresented in lagoon management strategies. Integrating functional indicators with delivery mode assessments can improve predictions of eutrophication risks and support more effective conservation planning in shallow coastal systems.

Keywords Nitrate pollution · Phytoplankton · Bacterioplankton · Zooplankton · Extracellular enzymatic activity · Pulse vs. continuous inputs

✉ Warren Meredith
wmeredith@icra.cat

Nuria Perujo
nuria.perujo-buxeda@ufz.de

María Antón-Pardo
m.teresa.anton@uv.es

Anna M. Romaní
anna.romani@udg.edu

Dani Boix
dani.boix@udg.edu

Jordi Compte
jordi.compte@udg.edu

María Bas-Silvestre
maria.bas@udg.edu

Xavier D. Quintana
xavier.quintana@udg.edu

Anna Menció
anna.mencio@udg.edu

[1] Catalan Institute for Water Research (ICRA), C. Emili Grahit 101, 17003 Girona, Spain

[2] Department of River Ecology, Helmholtz Centre for Environmental Research (UFZ), Magdeburg, Germany

[3] Institute of Aquatic Ecology, GRECO, University of Girona, 17003 Girona, Spain

[4] Cavanilles Institute of Biodiversity and Evolutionary Biology, University of Valencia, 46980 Paterna, Spain

[5] Grup de Geologia Ambiental I Aplicada (GAiA), Faculty of Sciences, Universitat de Girona, 17003 Girona, Spain

Introduction

Aquatic ecosystems worldwide are increasingly influenced by nutrient enrichment from both natural and anthropogenic sources (Lu and Tian 2017; De Vries 2021). Inputs from surface or groundwater runoff with nutrients from different origins (agriculture, wastewater, etc.) can alter ecosystem productivity, community composition, and biogeochemical cycling, often resulting in eutrophication and reduced ecological resilience (Cloern 2001). Beyond the total nutrient load, the temporal pattern of nutrient supply exerts strong control on ecosystem behavior. Whether nutrients arrive as short, concentrated surges or as continuous, low-level inflows determines how communities allocate resources and regulate productivity (Bernhardt and Palmer 2011). Ecological theory predicts that rapid, opportunistic taxa will dominate after discrete pulses, whereas more conservative, efficiency-oriented assemblages prevail under sustained inputs (Litchman and Klausmeier 2008). Despite these insights, relatively few experimental studies have explored the ecological consequences of nutrient delivery timing at the ecosystem scale.

Mediterranean coastal lagoons provide a naturally variable environment for understanding how nutrient delivery patterns influence ecological functioning. The hydrological cycle of these lagoons shifts seasonally between periods of flooding and high hydrological connectivity driven by rainfall and seawater inflows, and periods of dry-season confinement, during which reduced water exchange and intense evaporation lead to increased salinity (Badosa et al. 2006). These hydrological differences give rise to contrasting nutrient inputs that fluctuate in frequency and magnitude. Even though these lagoons may seem hydrologically isolated, subsurface inputs from adjacent aquifers become the main source of water renewal. These inflows typically transport nitrate at moderate concentrations, sustained through the dry months, and can represent a major fraction of total water exchange (Atkins et al. 2013; Cyronak et al. 2013; Meredith et al. 2022; Menció et al. 2023). Although nutrient levels appear modest, their persistence provides a steady enrichment capable of influencing planktonic activity. This steady input may sustain microbial productivity and gradually shift community composition, complicating efforts to distinguish natural variability from the early stages of anthropogenic eutrophication (Hutchinson, 1973; López-Flores et al. 2009). These observations underscore the need to better understand how sustained nutrient regimes shape plankton dynamics and influence long-term ecosystem trajectories.

To test these ideas, we carried out a controlled microcosm experiment in a Mediterranean lagoon using a resident plankton community. This study adopted a functional group approach focusing on phytoplankton, bacterioplankton, and zooplankton to examine how different nutrient delivery regimes shape planktonic dynamics. Each group represents a key trophic and biogeochemical role: primary production, microbial remineralization, and secondary consumption, respectively. The aim of this study was to examine how different time dynamics of nutrient inputs may influence the biomass contribution of the different planktonic groups and the heterotrophic activity linked to the use of carbon (C), nitrogen (N), and phosphorous (P) sources. We hypothesize that this community structure must be highly resilient to pulse type disturbances and adapted to the diminution of resource availability that occurs after them. However, these communities would be more sensitive to continuous nutrient inputs, usually of anthropogenic origin, and would maintain high productivity and high resource availability over time. Rather than focusing on taxonomic shifts, we also analyzed the extracellular enzyme activity (EEA) of the microcosms to help understand strategies adopted by planktonic organisms under different nutrient inputs. As EEA degrades complex molecules into more assimilable ones, it can be used as a proxy for microbial needs and acquisition of C, N, and P sources, thereby revealing functional shifts not apparent from abundance data alone. This framing allowed us to explore how the mode and frequency of nutrient delivery, rather than its total amount, may alter system-level processes relevant to lagoon resilience and management.

Materials and methods

Study site

The experiment was conducted in the La Pletera salt marshes, located in northeastern Iberia (42°02′00″N, 3°11′30″E). Microcosms were deployed within lagoon L04, which is a recently restored, permanent coastal lagoon characterized by high sediment permeability that ensures strong hydrological connectivity with the underlying aquifer (see Meredith et al. 2022 for more details). The salt marshes are shaped by a dynamic flooding–confinement regime, with episodic inputs from storm surges and rainfall during autumn and winter, and extended dry periods during summer (Badosa et al. 2006). Groundwater inputs into L04 prevents complete desiccation during warm seasons; however, evaporation and groundwater influx increase salinity during this period (Menció et al., 2017).

Experimental design

The experiment was carried out from 2 to 29 March 2020, a period characterized by increasing daylight, moderate temperatures, and favorable conditions for plankton development. A total of 20 polyethylene microcosms (8 L each) were positioned within plastic crates and deployed in Lagoon L04 at the La Pletera salt marshes (Fig. 1a). Each microcosm was assigned to one of four nutrient treatments, each replicated five times ($n=5$): control (no nutrient addition), pulse (episodic storm-driven nutrient input), continuous (sustained low-level subsurface inflow), and pulse–continuous (a combination of both delivery modes). Prior to the experiment, the lagoon's plankton composition was assessed to confirm homogeneity across potential experimental replicates (data not shown). The aim of the experiment was to evaluate how variations in nutrient delivery timing influence plankton dynamics, with specific attention to microbial and functional indicators.

All microcosms were deployed directly in the lagoon in rafts, spaced approximately 5 m apart to preserve ambient environmental conditions such as light and temperature. A pulley system using rods and ropes was used to limit physical disturbance from human access. To prevent the entry of external particles or organisms, each container was covered with a 4 mm mesh (Fig. 1b) (neck aperture ~30 mm). The microcosms were filled with lagoon water containing the native plankton community. Lagoon water was collected from a depth of 20–30 cm using a 1 L beaker from a kayak and transferred into four 20 L basins, which were then randomly distributed among the microcosms. Then, 3 L of water was removed from each container for initial zooplankton abundance and physico-chemical parameter analyses. The microcosms were then left to stabilize with 5 L of water for 3 days prior to nutrient additions, a period designated as days −3 to 0 in the sampling timeline to capture baseline conditions before experimental treatments began.

After 3 days, a volume of 2 L of artificial seawater (3.5% NaCl solution) was added to each microcosm to simulate a salinity pulse caused by a marine intrusion. The added seawater was tested and found to contain no detectable nitrate or phosphate. This represented a 40% volume increase and raised salinity to levels consistent with conductivity increases (~6 mS/cm) observed in La

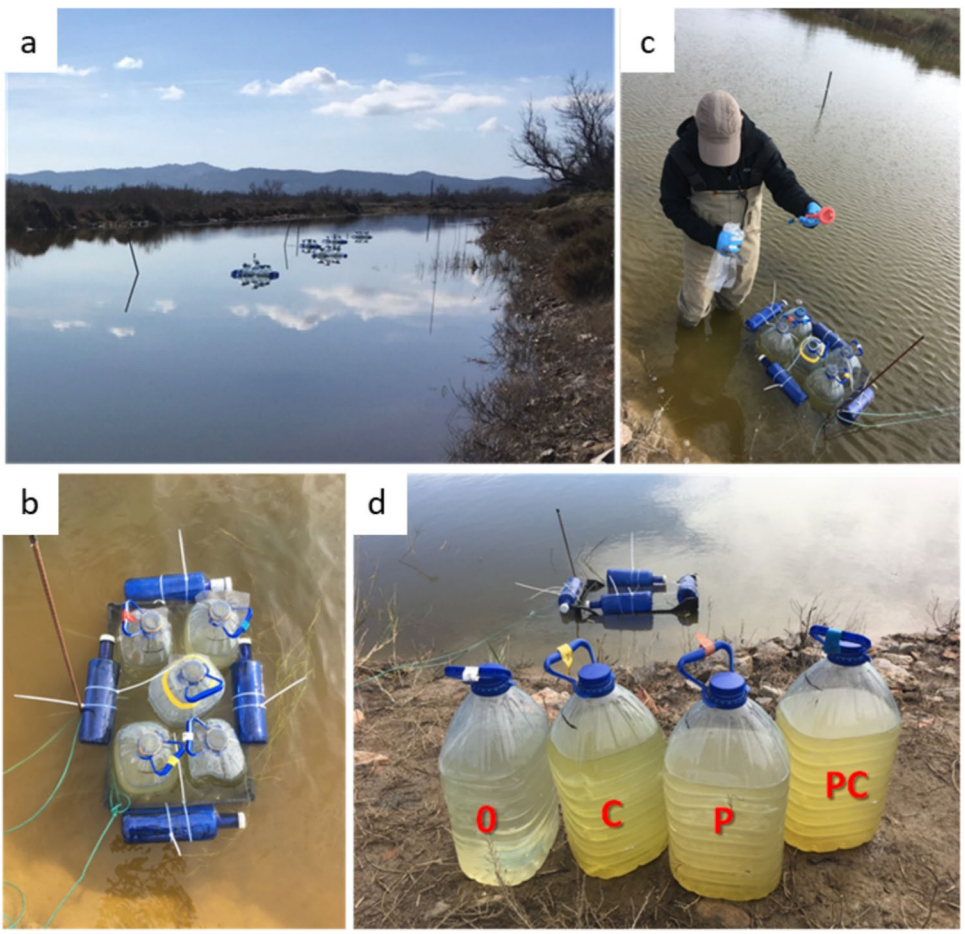

Fig. 1 Pictures of the microcosm setup in the L04 lagoon, within the La Pletera salt marshes. **a** Microcosms deployed in the lagoon. **b** Microcosm arrangements and flotation system, please note that an additional central microcosm was for analyzing zooplankton survival during the experiment (data not shown here). **c** Nutrient addition in the microcosms. **d** Visual appreciation of the different treatments: 0—control microcosm; C—continuous nutrient addition microcosm; P—pulse nutrient addition microcosm; PC—pulse–continuous addition microcosm

Pletera lagoons following storm events (Quintana et al., 1998b; Menció et al. 2023).

Nutrient additions began immediately after the artificial seawater additions and were subsequently administered daily at midday using sterilized glass pipettes (Fig. 1c). Each enriched microcosm received nutrient additions based on field-observed concentrations, while controls received distilled water. Detailed delivery regimes are described below. This approach enabled a direct comparison of delivery mode effects, independent of total nutrient quantity. Nutrient solutions were prepared in advance for each treatment and stored in clearly labeled containers, while the microcosms were clearly marked with distinct color codes to ensure accurate daily dosing and prevent cross-contamination (Fig. 1d). Although the experiment was originally scheduled to last 1 month, it concluded 4 days earlier owing to coronavirus disease 2019 (COVID-19) restrictions.

Nutrient additions

To simulate realistic nutrient enrichment scenarios, sodium nitrate ($NaNO_3$) and dipotassium phosphate (K_2HPO_4) were used as inorganic sources of nitrogen and phosphorus. Target cumulative concentrations were based on the highest levels recorded in nearby irrigation canals and lagoon waters following storm events, which were approximately 17 mg/L NO_3^- and 1.48 mg/L PO_4^{3-} (Menció et al. 2023), with a molar N:P ratio of ~16:1. This is consistent with field observations that indicate that phosphorus is not typically limiting in the La Pletera lagoons (Boadella et al. 2021). These total concentrations were divided across treatments on the basis of their respective delivery regimes to allow for direct comparison of mode-specific effects. The control received equivalent volumes of distilled water on subsequent days, while the pulse treatments received the same after the total nutrient addition to ensure consistent handling across all treatments.

The preparation of the nutrient concentrations is as follows:

- Control: Received 10 mL of distilled water each day, with no added nutrients.
- Continuous: Each microcosm was dosed with 10 mL/day of a low-concentration nutrient solution, formulated by dissolving 0.583 g $NaNO_3$ and 0.075 g K_2HPO_4 in 1 L of distilled water (equivalent to 0.61 mg/L NO_3^- and 0.05 mg/L PO_4^{3-} per dose).
- Pulse: A single high-dose nutrient addition was applied on day 0 (10 mL), prepared by dissolving 3.266 g $NaNO_3$ and 0.418 g K_2HPO_4 in 200 mL distilled water (yielding 17 mg/L NO_3^- and 1.48 mg/L PO_4^{3-}). From day 1 onward, these microcosms received 10 mL/day of distilled water only.
- Pulse–continuous: On Day 0, microcosms were given a half-strength pulse dose (5 mL of the pulse solution + 5 mL distilled water). For Days 1–24, they received 10 mL/day of a 1:1 diluted version of the continuous treatment solution, prepared by dissolving the same nutrient quantities in 2 L of distilled water.

To apply the nutrient additions to the microcosms, 10 mL pipettes were used.

Sampling and analyses of water characteristics

Field measurements of temperature, conductivity, pH, and dissolved oxygen (DO) were taken directly in the microcosms on the initial (day −3) and final day (day 24) using portable multiparameter instruments (Crison CM35, WTW-330i, Crison OXI45). Water samples were collected using 25 mL glass pipettes during eight sampling campaigns: day −3 (initial conditions during microcosm filling), day 0a and day 0b (corresponding to before and after nutrient additions), and days 1, 5, 11, 19, and 24. These were collected to capture baseline conditions and track planktonic and biogeochemical responses to nutrient treatments over time. After collection, samples were transferred into 250 mL amber glass bottles, kept in darkness at 4 °C until laboratory analysis. Carbonate and bicarbonate concentrations (100 mL samples) were determined by Gran titration, achieving a relative standard deviation (RSD%) of < 1%, and used to estimate total inorganic carbon. Dissolved organic carbon (DOC) in filtered 50 mL samples was analyzed by catalytic oxidation (RSD% < 1%). Samples for major ions (15 mL) and inorganic nutrients (NO_2^-, NO_3^-, NH_4^+, PO_4^{3-}) (50 mL) were sterilized by filtration through 0.22 µm polyethersulfone (PES) syringe filters (Filter-Lab®, Spain). Ammonium concentrations were quantified by ion chromatography (Thermo Scientific Dionex ICS-5000; RSD% 2.82%), and spectrophotometry was used to measure total phosphorus (TP), nitrate, nitrite, and phosphate (RSD% 2.82%, 2.44%, and 3.42%, respectively). Total nitrogen (TN) was determined using a total organic carbon (TOC) analyzer (TOC-V CSH, Shimadzu). Analytical quality control was verified by ionic mass balance, with sample errors below 5%. Organic nitrogen (N_{org}) and phosphorus (P_{org}) were estimated as the difference between total and inorganic fractions. Analyses were conducted using 100 mL water samples, divided into appropriate subsample volumes. The corresponding concentrations of organic carbon, nitrogen, and phosphorus (including DOC) were converted to molar units and used to calculate C:N, N:P, and C:P ratios, which describe the relative composition of organic matter across treatments.

Phytoplankton and bacterioplankton biomass and specific growth rate, and zooplankton biomass

Water samples were collected from each microcosm to determine the abundance and biomass of pico- and nano-phytoplankton (autotrophic organisms) and bacterioplankton (heterotrophic organisms). For microbial cytometry, 1.5 mL subsamples were fixed with 1% paraformaldehyde and 0.05% glutaraldehyde, flash-frozen in liquid nitrogen, and stored at –80 °C until analysis. After thawing, phytoplankton and bacterioplankton were analyzed using a FACScalibur flow cytometer (BD Biosciences) equipped with a 488 nm laser, following protocols adapted from López-Flores et al. (2009) and Gasol and Del Giorgio (2000).

Phytoplankton populations were identified on the basis of forward scatter (FSC) and red autofluorescence (FL3). A 2 µm yellow-green bead solution (molecular probes) was used as an internal standard, and FSC values were calibrated against known culture volumes using bead-normalized regression curves. This approach targets cells < 20 µm in size, excluding larger microphytoplankton.

Bacterioplankton samples were stained with SYTO 13 (final concentration 2 µM), protected from light, and analyzed on the basis of side scatter (SSC) and green fluorescence (FL1). A 1 µm bead solution (Polysciences) was used for normalization. Biomass estimates were derived from biovolume and abundance, using the conversion factors and protocols described in Troussellier et al. (1999) and Gasol and Del Giorgio (2000). Specific growth rate (µ/d) is expressed as the rate of production of biomass per unit time, per unit initial concentration of biomass and calculated as:

$$\mu = \frac{N_1 - N_0}{N_0(t_1 - t_0)}$$

where N_1 is the biomass of phytoplankton or bacterioplankton at time t_1. N_0 is the initial biomass and t_0 is the initial time. While this estimate is based on cytometrically derived biomass, which has known limitations (e.g., in biovolume calibration), it provides a consistent basis for comparing growth patterns across treatments.

Zooplankton samples were collected on day −3, after the distribution of lagoon water into the different microcosms, and on day 24 after samples were taken. A total volume of 3 L was collected from each microcosm, filtered through a 50 µm net, and preserved in 4% formalin. The sample volume was sufficient to estimate zooplankton biomass in this high-productivity system based on prior work by Quintana et al. (2021). We followed the same protocol as the authors for zooplankton counting and biomass estimations, focusing on metazoan zooplankton within the 50–500 µm size range, including rotifers, copepods, and cladocerans.

Extracellular enzyme activity

Three extracellular enzyme activities (EEA) were measured: β-glucosidase (GLU) (EC 3.2.1.21), leucine aminopeptidase (LAP) (EC 3.4.11.1), and phosphatase (AP) (EC 3.1.3.1–2), which degrade simple polysaccharides, peptides, and organic phosphorus compounds, respectively (Romaní et al. 2012). Fresh samples were incubated with fluorescent-linked artificial substrates at 0.3 mM saturation concentration for 1 h at 20 °C in dark conditions, following (Boadella et al. 2021). At the end of the incubation, fluorescence was measured (Tecan, Infinite M200 PRO microplate reader). Results are given as µmol methylumbellyferone (MUF)/L/h or µmol AMC (aminomethylcoumarin)/L/h. Samples were collected up to day 19. Samples for day 24 were not possible due to COVID-19 restrictions.

Data analysis

Differences between the microcosm treatments on the final day for DO, organic nutrients, pH, temperature, and conductivity were analyzed using one-way analysis of variance (ANOVA), followed by Tukey's HSD post hoc test when significant effects were detected.

For EEA, significant differences between treatments at each sampling date, as well as significant differences between sampling dates were analyzed using two-way ANOVA. To account for the variation in the initial biomass of phytoplankton and bacterioplankton of each of the microcosms before the addition of nutrient treatments, a linear mixed-effect model (LME; Lindstrom and Bates 1988) was used with the individual microcosms as a random term in the LME model. To evaluate the effect of treatment and time (sampling day) on plankton biomass, a two-way analysis of covariance (ANCOVA) was conducted separately for phytoplankton and bacterioplankton. For each analysis, the biomass of the other group was included as a covariate (e.g., phytoplankton with bacterioplankton as covariate) to account for potential interactions and isolate treatment effects. To further examine treatment effects over time, a simple main effects analysis was conducted for each sampling day using ANCOVA. In addition, pairwise comparisons between sampling days within each treatment were performed to assess temporal dynamics. Nutrient uptake was estimated from the difference between cumulative nutrient additions and measured nutrient concentrations in the microcosms over time, with the assumption that decreases in dissolved nutrient concentrations reflected assimilation or removal by the planktonic community. Differences between treatments and sampling days for nitrate and phosphate uptake, as well as phytoplankton and bacterioplankton growth rates, were analyzed using two-way ANOVA, with post hoc comparisons using the

Bonferroni correction. Due to the extensive number of statistical tests, detailed significance values are reported in the "Results" section and full statistical outputs are provided in the Supplementary Material.

Linear regression was used to test whether phytoplankton or bacterioplankton biomass significantly predicted zooplankton biomass from the initial and final day of the experiment; that included five replicas for phytoplankton, bacterioplankton, and zooplankton ($N = 10$) to examine whether shifts were caused by bottom-up or top-down effects (McQueen et al. 1986). Prior to analysis, the assumptions of linear regression were evaluated by inspecting residual distributions using Q–Q plots and residual versus fitted plots, and normality of residuals was assessed using the Shapiro–Wilk test. No significant deviations from normality were detected in any of the models ($p > 0.05$). This approach was used in an exploratory capacity to assess whether directional trends in planktonic biomass could provide insight into trophic linkages under different nutrient delivery regimes. All variables were log-transformed. A significance level of 0.05 was used for all statistical tests. All statistical analyses were completed with R software (R Core Team 2021) and the jamovi project (2021) (jamovi Version 2.2.2, Computer Software, retrieved from https://www.jamovi.org). The experimental design and analytical procedures followed the same general setup described in Meredith et al. (2025), with modifications detailed above.

Results

Water quality parameters of the microcosms on the initial day (day −3) and final day (day 24)

The summary of the water quality parameters of each of the treatments is shown in Table 1 for the initial and final day of the experiment, spanning 24 days. While conductivity increased by ~6 mS/cm in all the treatments, the control treatment showed moderate increases in pH and dissolved oxygen (DO), along with a small reduction in alkalinity and total inorganic carbon (TIC). Ammonium (NH_4^+) concentrations declined slightly by the final day, and molar C:N, N:P, and C:P ratios remained relatively high in the control.

In contrast, the nutrient-enriched treatments (pulse, continuous, and pulse–continuous) showed more pronounced changes. All exhibited a twofold increase in pH compared with the control, alongside significant increases in DO. The most substantial DO increase occurred in the continuous treatment (+89%), followed by pulse–continuous (+64%), and pulse (+52%) (one-way ANOVA, $p < 0.001$). These treatments also had greater decreases in alkalinity and TIC than the control. All nutrient-enriched treatments showed reduced NH_4^+ concentrations by day 24. Also, molar N:P and C:P ratios declined threefold to fourfold relative to the control. Organic matter concentrations (DOC, N_{org}, P_{org}) were significantly higher in the

Table 1 Initial day (day −3) and final day (day 24) of water quality and nutrient concentrations (mean ± SD) within each microcosm treatment of control, continuous, pulse, and pulse–continuous ($n = 5$)

Treatment/day	Control		Continuous		Pulse		Pulse–continuous	
	Initial	Final	Initial	Final	Initial	Final	Initial	Final
Temperature (°C)	14.8	13.5 ± 0.2	14.8	13.7 ± 0.1	14.8	13.7 ± 0.1	14.8	13.8 ± 0.1
Conductivity (mS/cm^{-1})	15.1	21.9 ± 0.2	15.1	21.9 ± 0.4	15.1	21.8 ± 0.3	15.1	21.8 ± 0.2
pH	6.6	8.8 ± 0.1	6.6	10.2 ± 0.1	6.6	10.1 ± 0.0	6.6	10.1 ± 0.1
Dissolved oxygen (%)	97.9	105.8 ± 3.9^{a}	97.9	184.8 ± 4.9^{b}	97.90	148.8 ± 3.9^{c}	97.9	160.2 ± 5.3^{d}
NH_4^+ (mg/L^{-1})	0.58 ± 0.2	0.03 ± 0.0	0.36 ± 0.2	0.10 ± 0.1	0.28 ± 0.1	0.03 ± 0.01	0.28 ± 0.1	0.03 ± 0.01
Alkalinity (mg/L $CaCO_3$)	275.2 ± 8.9	221.7 ± 7.3	282.9 ± 8.9	148.6 ± 6.3	273.34 ± 5	145.1 ± 6.8	271.9 ± 12.7	137.8 ± 4.2
TIC (mg/L^{-1})	270.3 ± 8.5	207.7 ± 5.8	276.7 ± 9.9	109.2 ± 6.4	266.4 ± 4.4	111.3 ± 5.9	265.9 ± 11.6	105.9 ± 2.1
DOC (mg/L^{-1})	21.9 ± 0.7	17.6 ± 1.1^{a}	21.4 ± 0.6	20.9 ± 0.7^{b}	22.13 ± 0.5	19.9 ± 0.4^{c}	21.5 ± 0.9	20.6 ± 0.3^{b}
N_{org} (mg/L^{-1})	1.86 ± 0.2	1.36 ± 0.2^{a}	1.97 ± 0.1	3.14 ± 0.2^{b}	1.89 ± 0.1	2.75 ± 0.2^{c}	1.95 ± 0.1	3.15 ± 0.1^{b}
P_{org} (mg/L^{-1})	0.08 ± 0.05	0.06 ± 0.01^{a}	0.07 ± 0.02	0.29 ± 0.02^{b}	0.07 ± 0.03	0.25 ± 0.01^{c}	0.08 ± 0.03	0.29 ± 0.02^{b}
Molar C:N	13.8 ± 1.3	15.2 ± 1.9	12.6 ± 0.7	7.9 ± 0.6	13.6 ± 0.3	8.3 ± 0.9	12.8 ± 0.8	7.6 ± 0.4
Molar N:P	56.6 ± 20.5	49.7 ± 5.9	65.6 ± 16.1	24.2 ± 2.1	60.5 ± 16.2	23.4 ± 1.3	55.9 ± 19.0	24.4 ± 0.7
Molar C:P	764.4 ± 232.5	755.6 ± 127.2	820.4 ± 170.8	191.3 ± 10.1	824.5 ± 227.8	194.5 ± 21.1	709.6 ± 206.6	186.3 ± 10.8

Temperature, conductivity, pH, and dissolved oxygen on the initial day were measured from the same water collected to distribute to the different microcosms. Results with the same letters are not significantly different between treatments on the final day (day 24) (one-way ANOVA, $p < 0.001$)

continuous and pulse–continuous treatments compared with the control and pulse treatments (one-way ANOVA, $p < 0.001$).

Nitrate and phosphate concentrations

Nitrate levels in the control remained low throughout the experiment (0–0.3 mg/L), with only distilled water added (Fig. 2a). The continuous treatment showed a moderate increase in nitrate following daily additions of 0.6 mg/L, peaking around day 2 (~0.65 mg/L), but declined to < 0.2 mg/L by the end (Fig. 2b). The pulse treatment reached its maximum (17 mg/L) on day 0, followed by a sharp decline of 70% loss by day 11 and near-complete depletion by day 19 (Fig. 2c). The pulse–continuous treatment showed a similar pattern at half the concentration, with an 81% decline by day 11 and low levels maintained thereafter (Fig. 2d), reflecting combined dynamics of both regimes.

Phosphate concentrations followed a similar pattern. The control and continuous treatments converged to comparable levels by day 24 (Fig. 3a, b). The pulse–continuous treatment showed early depletion before day 5, while the pulse treatment exhibited a 65% decline in phosphate between days 5 and 11 (Fig. 3c, d), with low concentrations persisting in all treatments thereafter.

Phytoplankton and bacterioplankton biomass: specific growth rate and nutrient uptake rates

Results from the linear mixed-effect model with the individual microcosms as a random term indicated that the percentage of variance explained by the microcosm variable was 5.4×10^{-7}, signifying no difference between replicates at the beginning of the experiment. The interaction between treatment and time (day) on bacterioplankton and phytoplankton biomass was statistically significant (two-way ANCOVA, $F(15, 95) = 6.78$, $p < 0.001$). The effect of treatments on phytoplankton and bacterioplankton biomass was statistically significant on days 5, 11, and 19, but not significant on days 0 and 1 (Supplementary Material Table S1). However, significant increases in phytoplankton biomass occurred at different rates in the nutrient addition microcosms on day

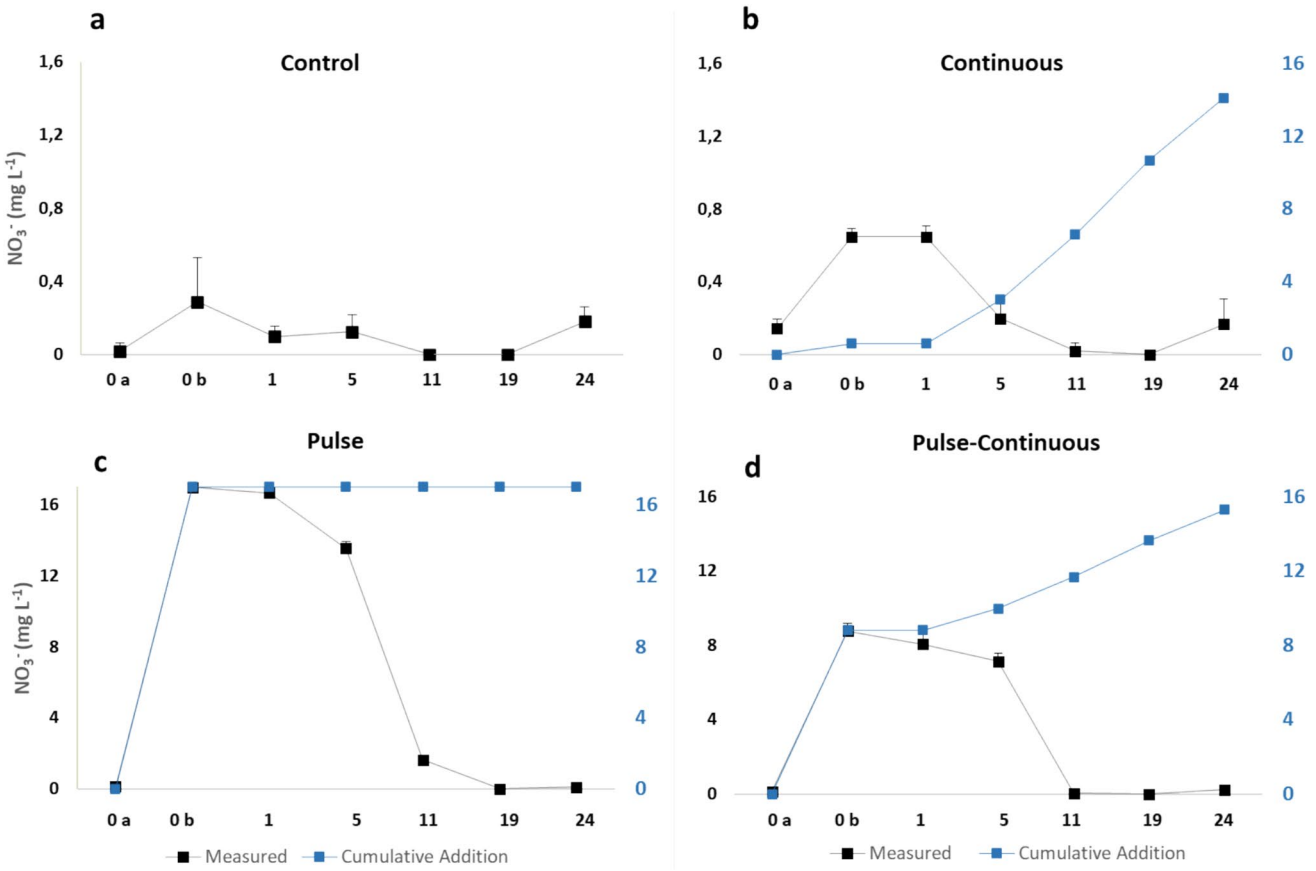

Fig. 2 Accumulated nitrate additions (blue) (right *y*-axis) and measured nitrate levels (black) (left *y*-axis) averaged (mean ± SD) within each of the nutrient treatments of control (**a**), continuous (**b**), pulse (**c**), and pulse–continuous (d). Total nitrate additions for all treatments, except control, were 17 mg/L for the duration of the experiment. Day 0a indicates nutrient level before additions and day 0b after additions

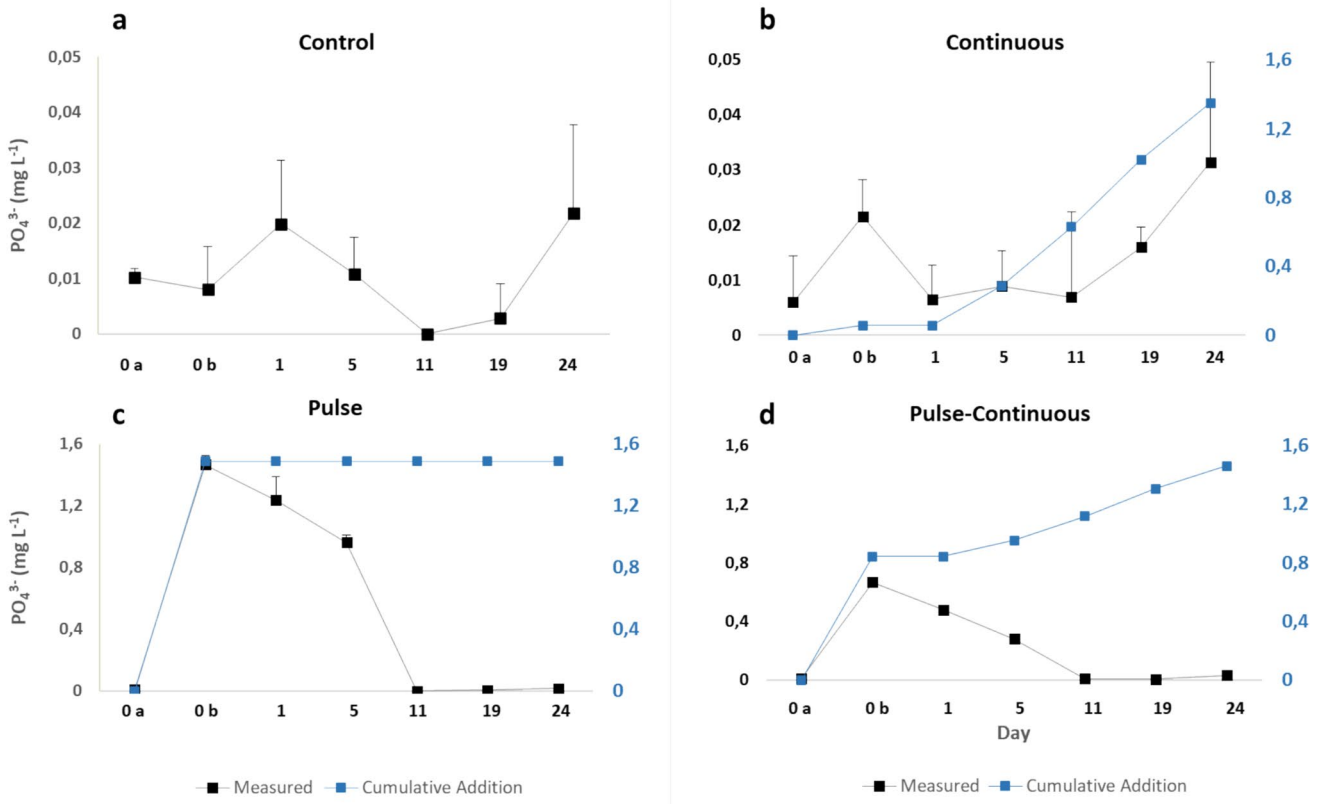

Fig. 3 Accumulated phosphate additions (blue) (right *y*-axis) and measured phosphate levels (black) (left *y*-axis) averaged (mean ± SD) within each of the nutrient treatments of control (**a**), continuous (**b**), pulse (**c**), and pulse–continuous (**d**) along the duration of the experiment. Total planned phosphate level for all treatments was 1.48 mg/L for the duration of the experiment. Note measured concentration levels in a and b (black) are ten orders of magnitude lower than in c and d (black). Day 0a indicates nutrient level before additions and day 0b after additions

11, except for the pulse and pulse–continuous microcosms, which were not statistically different in biomass accumulation. The phytoplankton biomass continued to increase in the continuous treatments by day 19 and was significantly higher than the pulse–continuous phytoplankton biomass. The phytoplankton biomass increased in both pulse and pulse–continuous treatments by day 24, and although they were not significantly different between each other, they both were significantly higher than the continuous treatments.

Bacterioplankton biomass was not significantly different between the microcosms on day 0, day 1, and day 5 (Fig. 4b; Supplementary Material Table S2). However, significant increases in bacterioplankton biomass occurred on day 11, with the pulse treatment significantly higher than the control and the continuous treatments and only marginally higher than the pulse–continuous treatments. Bacterioplankton biomass continued to increase in the continuous treatments on day 24 and was significantly higher than the pulse and pulse–continuous treatments. Both pulse and pulse–continuous treatments saw more than a 76% decline in biomass and were not statistically different to the biomass in the control by day 24. Throughout the entire experiment, there were no significant changes in biomass fluctuations between day 0 and day 24 for both phytoplankton and bacterioplankton biomass in the control microcosms (Supplementary Material Table S3 and Table S4).

Specific growth rate for phytoplankton was not significantly different between day 0 and day 1 for all the treatments (Fig. 4c; Supplementary Material Table S5). However, the continuous treatment's specific growth rates were significantly higher than the pulse and pulse–continuous treatments on day 5 of the experiment and again on day 19. On day 11, the pulse–continuous treatments had the highest specific growth rate of all the microcosms and significantly higher than the pulse treatments. This trend continued on day 24; however, both pulse and pulse–continuous specific growth rates were not significantly different from each other. Bacterioplankton specific growth rate did not see significant differences between microcosms from day 0 to day 1, and on day 5 between the pulse and pulse–continuous treatments (Fig. 4d; Supplementary Material Table S6), although they were significantly higher than the continuous treatments.

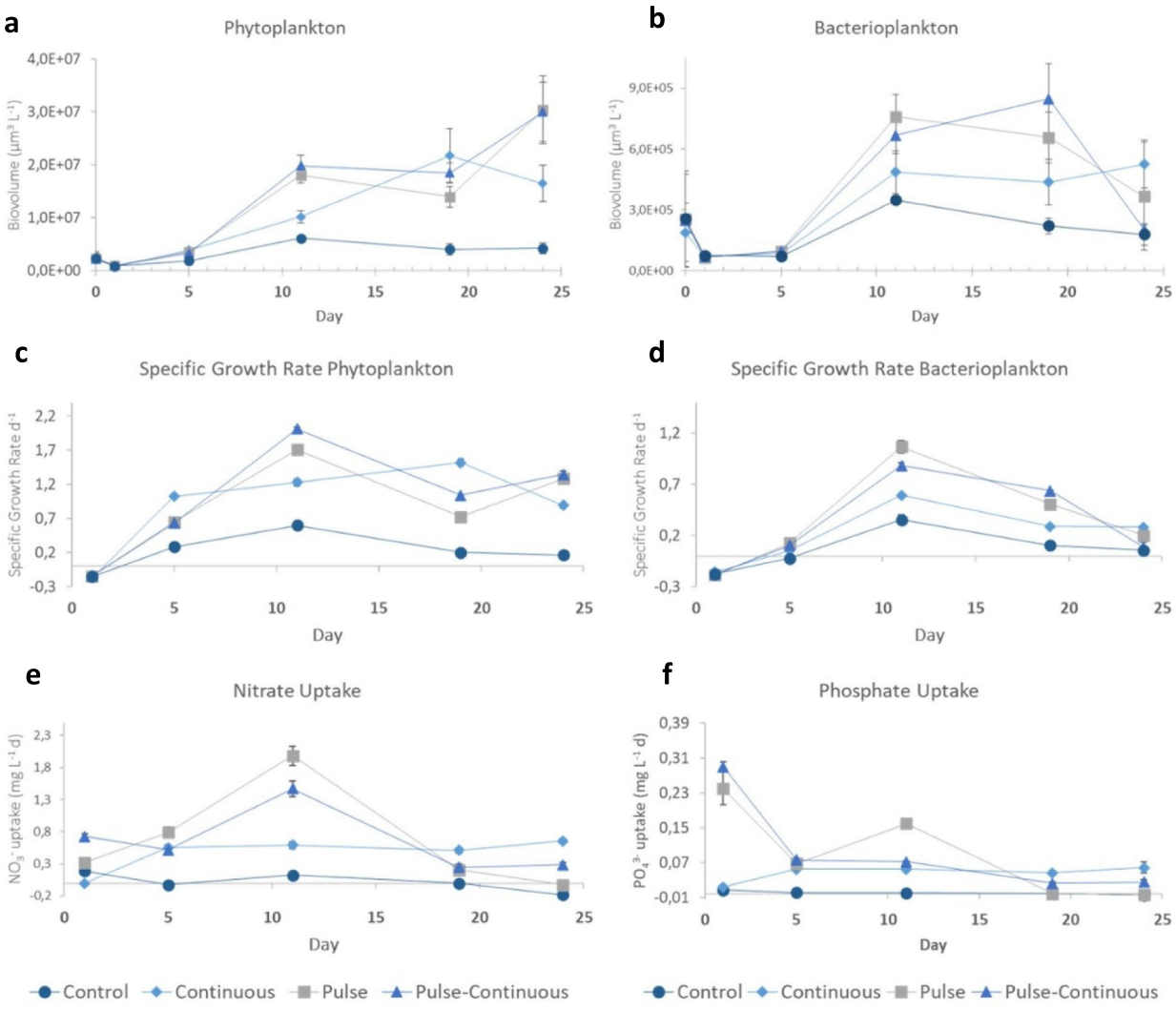

Fig. 4 Biomass fluctuations of phytoplankton (**a**) and bacterioplankton (**b**) expressed as biovolume from the initial day 0 to day 24. Specific growth rate per day of phytoplankton (**c**) and bacterioplankton (**d**), as well as nitrate uptake (**e**) and phosphate uptake (**f**) per sampling day according to the nutrient treatment regimes of control, continuous, pulse and pulse–continuous

There was a general decline in specific growth rate in all the treatments on day 19, although the continuous treatments were significantly higher than the pulse and pulse–continuous treatments on day 24.

Nitrate uptake was significantly different in all the treatments on day 1, with the continuous treatments higher than the pulse treatments (Fig. 4e; Supplementary Material Table S7). However, day 5 saw the pulse treatment increase in uptake and significantly higher than the continuous and pulse–continuous treatments. This trend continued to day 11; however, the pulse–continuous was significantly higher in uptake than the continuous treatment. Nitrate uptake dropped for both the pulse and pulse–continuous treatments on day 19 and day 24 and resulted in significantly lower than the continuous treatments; however, the pulse–continuous remained significantly higher than the pulse treatments on day 24. Phosphate uptake was also significantly different in all the treatment microcosms on day 1 (Fig. 4f; Supplementary Material Table S8); however, the pulse treatment was significantly higher in uptake than the continuous and pulse–continuous treatments on day 11. Also, the pulse treatment dropped significantly to similar levels of the control and pulse–continuous treatments on day 19. This trend continued on day 24; however, the pulse treatment was significantly lower than the pulse–continuous treatment on this day.

Phytoplankton and bacterioplankton biomass influence on zooplankton biomass

Zooplankton biomass was initially similar across all treatments, but differences between treatments were observed in the final sampling (Fig. S2). Relative to initial conditions, zooplankton biomass was 50% higher in the control treatment and 67% higher in the continuous treatment, while the pulse–continuous treatment showed a 32% higher biomass. In contrast, zooplankton biomass in the pulse treatment was 58% lower than initial values (Fig. S2). Regression analyses (Table 2) revealed significant positive relationships between zooplankton biomass and both phytoplankton and bacterioplankton in the continuous treatment ($R^2 = 0.56$ and 0.73, respectively; $p < 0.05$), suggesting a bottom-up control. The control treatment showed a weaker but significant relationship with bacterioplankton only, while no significant predictors were found in the pulse–continuous treatment. Notably, the pulse treatment showed a negative correlation between zooplankton and phytoplankton biomass ($R^2 = 0.65$; $p < 0.05$), indicating the absence of a bottom-up control.

Extracellular enzyme activity

The hydrolytic activities of LAP and GLU increased overall with nutrient additions over the experiment duration and irrespective of nutrient load received after 5 days (Fig. 5). However, GLU activity was significantly lower in the pulse treatments on the last 2 days than the other nutrient-enriched treatments (Fig. 5 **b**; two-way ANOVA, $p < 0.05$). Although results are variable over time, the pulse–continuous treatments had higher LAP activity on day 19 than the pulse treatment (Fig. 5a; two-way ANOVA, $p < 0.001$), and marginally higher in the continuous treatment (Fig. 5a; two-way ANOVA, $p = 0.06$). GLU activity was significantly higher in the continuous and pulse–continuous treatments than the pulse on the final 2 days (Fig. 5b; two-way ANOVA, $p < 0.001$). The control showed low activity of LAP and GLU from day 5 until the end of the experiment. Differences between treatments for AP activity appeared on day 5, with higher values in control and continuous treatments than in the pulse and pulse–continuous treatments. On days 11 and 19, only the control treatment showed fivefold higher activity than the three nutrient-enriched treatments.

Discussion

Our findings suggest that the temporal pattern of nutrient delivery, rather than concentration alone, reshapes community functioning and biogeochemical dynamics. Low-level but persistent nutrient supply maintained elevated microbial activity even at moderate concentrations, highlighting the importance of both nutrient quantity and delivery mode in aquatic ecosystems prone to diffuse, sustained enrichment.

This functional group framework, which represents primary production, microbial remineralization, and secondary consumption, provides a useful way to examine bottom-up control, nutrient cycling, and early signs of eutrophication. While finer taxonomic or trait-based resolution could enhance ecological interpretation, the functional grouping remains appropriate given the scale of the study. Notably, extracellular enzyme activity (EEA) complemented biomass measurements by revealing microbial nutrient acquisition strategies that are otherwise difficult to detect. Although microphytoplankton were not included, the focus on pico- and nanophytoplankton is consistent with previous studies showing that these groups typically dominate under spring conditions in Mediterranean lagoons (López-Flores et al., 2006).

Nutrient regime effects on biomass dynamics and microbial function

Biomass dynamics showed distinct temporal responses to nutrient regimes. Phytoplankton and bacterioplankton increased early in the experiment but diverged thereafter. Pulse and pulse–continuous additions triggered a rise in bacterioplankton biomass, followed by a decline, likely due to nutrient depletion after rapid phosphate uptake. In contrast,

Table 2 Linear regression analysis to test phytoplankton and bacterioplankton biomass influence on zooplankton biomass from the initial to final day

Treatment	Relationship	Estimate	SE	*t*	*p*-Value	R^2
Control	Zooplankton ~ phytoplankton	0.06	0.03	1.93	0.09	0.32
	Zooplankton ~ bacterioplankton	2.90	0.78	3.7	0.01*	0.63
Continuous	Zooplankton ~ phytoplankton	0.03	0.01	2.75	0.03*	0.56
	Zooplankton ~ bacterioplankton	1.33	0.33	4.07	0.01*	0.73
Pulse	Zooplankton ~ phytoplankton	−0.02	0.01	−3.59	0.01*	0.65
	Zooplankton ~ bacterioplankton	−1.20	0.70	−1.71	0.13	0.3
Pulse–continuous	Zooplankton ~ phytoplankton	0.01	0.01	1.04	0.33	0.15
	Zooplankton ~ bacterioplankton	2.24	2.46	0.91	0.39	0.12

*Significance at the 95% confidence interval

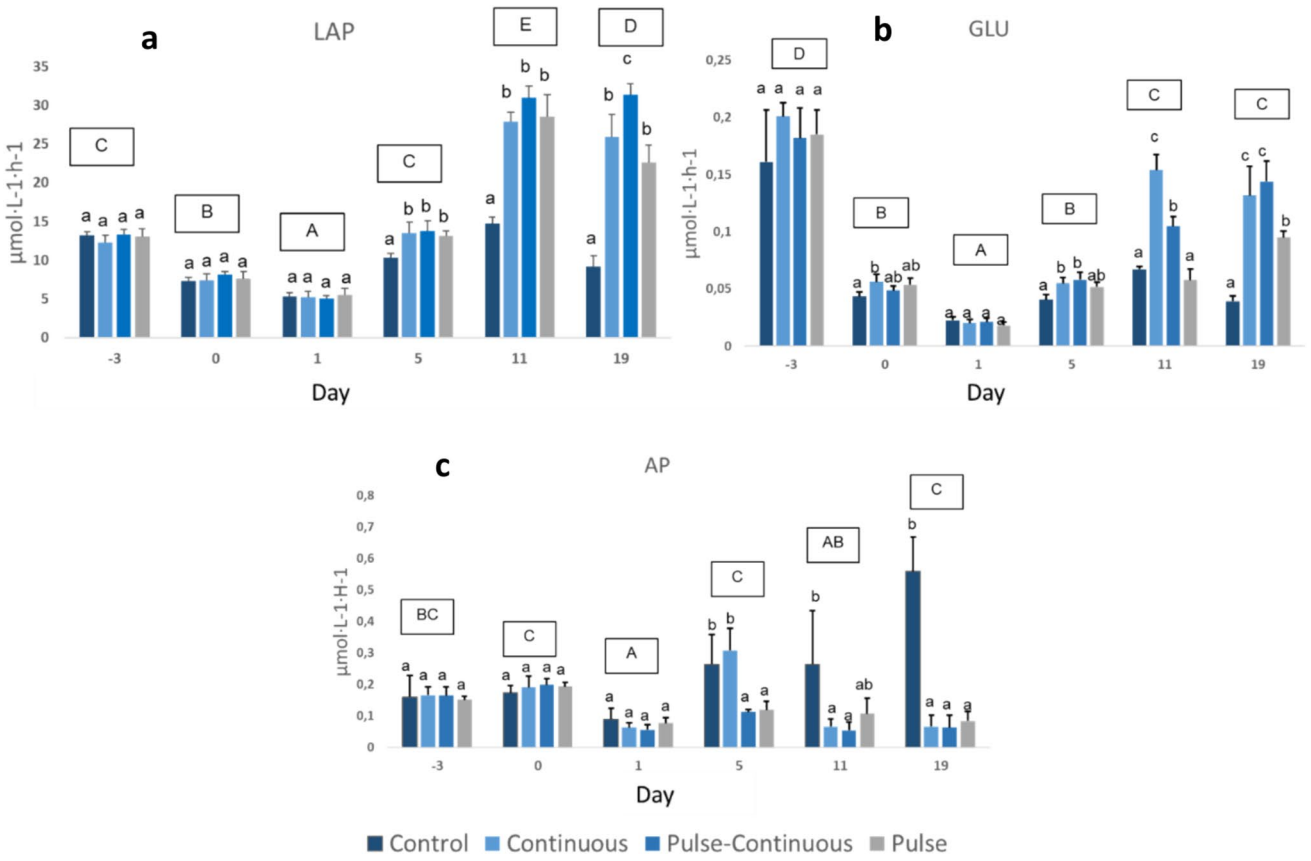

Fig. 5 Extracellular enzyme activity of leucine aminopeptidase (LAP) (EC 3.4.11.1) (**a**), β-glucosidase (GLU) (EC 3.2.1.21) (**b**), and phosphatase (AP) (EC 3.1.3.1–2) (**c**) of all the microcosms from the initial conditions prior to nutrient additions (day −3) to day 19 of the experiment. Lower-case letters indicate significant differences between treatments at each sampling date ($p < 0.05$), and upper-case letters indicate significant differences between sampling dates ($p < 0.05$), two-way ANOVA

continuous inputs supported sustained growth across all functional groups, indicating consistent bottom-up control over the 24-day period (Fig. S4). These contrasting trajectories likely stem from the differential phosphorus demands of heterotrophs and autotrophs (Vadstein 2000; Cabrerizo et al. 2019). In the pulse treatments, early bacterial dominance may have temporarily suppressed phytoplankton growth, with subsequent nutrient recycling facilitating phytoplankton recovery by day 24. This is supported by lower DOC and TIC levels at the end of the experiment and suggests high microbial turnover and carbon demand. This interpretation is also supported by the biomass trends shown in Fig. 5, where sustained phytoplankton growth in the continuous treatment corresponded with higher final-day DO levels. Although both the pulse and pulse–continuous treatments maintained DO above saturation, final-day levels were lower in the pulse treatment (Table 1), likely from higher initial microbial respiration and slower oxygenic production recovery. This suggests that DO trends reflect not only nutrient availability but also the interaction between autotrophic production and heterotrophic demand. This trend was paralleled by pH increases across all treatments, with the greatest rise observed under continuous enrichment. This is consistent with elevated photosynthetic activity and CO_2 uptake during plankton blooms, a common driver of pH elevation in productive aquatic systems. These shifts may also reflect quorum sensing processes, such as bacterial signaling dependent on cell density and nutrient availability that can be downregulated following post-pulse declines in biomass, thereby modulating community interactions and influencing phytoplankton succession (Miller and Bassler 2001; Urvoy et al. 2022).

The observed lower zooplankton biomass in pulse treatments (despite rising phytoplankton) further highlights potential trophic mismatches. This pattern suggests that phytoplankton produced under pulsed regimes may have been of lower nutritional quality or poorly timed relative to zooplankton feeding requirements. Similar outcomes have been reported elsewhere, where pulsed nutrient additions led to the dominance of inedible or nutrient-poor phytoplankton (Butzler and Chase 2009). It should also be noted that microzooplankton (e.g., ciliates and heterotrophic dinoflagellates)

were not included in the zooplankton component analyzed here, although these groups can play an important role in mediating trophic interactions between phytoplankton and higher consumers in planktonic food webs. Under continuous enrichment, phytoplankton growth persisted and zooplankton biomass also remained higher, pointing to more stable and trophically favorable conditions. Ultimately, on an ecologically relevant time scale, ranging from weeks to months depending on retention time and hydrology, sustained low-concentration nutrient inputs can shift lagoon functioning. While not triggering overt eutrophication symptoms, they may alter community structure and reduce resilience (Cloern 2001). Though, in nutrient-limited settings such as Mediterranean lagoons, they may also support productivity (García-Robledo et al. 2016; Viaroli et al. 2008). Overall, shifts toward greater importance of microbial components within planktonic food webs, modified trophic balance, and reduced ecosystem resilience may escape detection if monitoring focuses only on nutrient concentrations (Carstensen et al. 2011). In the context of the La Pletera, nitrate concentrations around 17 mg/L were moderate but still sufficient to elicit clear microbial responses. This interpretation is supported by previous work (Svensen et al. 2002), which showed that continuous nutrient supply favors organic matter retention and trophic stability, while pulsed inputs promote biomass export. The intermediate patterns observed in the pulse–continuous treatment further suggest additive or interacting effects of both regimes on plankton dynamics. These patterns likely reflect underlying differences in how microbial communities respond to resource availability. Bacterioplankton and phytoplankton, while both responding to nutrient supply, exhibit distinct ecological strategies. Bacterioplankton often thrive under high dissolved organic carbon and phosphorus-limited conditions, whereas phytoplankton depend more on inorganic nitrogen and phosphorus (Redfield 1958; Vadstein 2000; Sarmento and Gasol 2012; Sörenson et al. 2020). These differences in resource requirements and uptake capabilities help explain the divergent biomass trajectories and enzyme activity patterns observed across the nutrient regimes. These differences, along with the higher nutrient uptake efficiency and lower cellular requirements of bacteria due to their small size (Thingstad and Lignell 1997; Litchman et al. 2015), help explain the early bacterial dominance in pulse treatments and the sustained autotrophic activity in continuous regimes. Our results are consistent with these functional expectations and underscore the importance of nutrient delivery patterns in shaping trophic structure.

Finally, enzyme activity patterns provide complementary evidence of nutrient limitation and community strategy. GLU and LAP activity increased in nutrient-enriched microcosms, indicating microbial demand for carbon and nitrogen, respectively. These enzymes are involved in breaking down polysaccharides (GLU) and peptides (LAP), reflecting enhanced organic matter processing (Arnosti 2011). In contrast, consistently low alkaline phosphatase activity suggested that phosphorus remained non-limiting. This interpretation is consistent with high LAP:AP ratios previously observed in Mediterranean lagoons (Boadella et al. 2021). Heterotrophic bacteria, with their lower N:P stoichiometry (Cleveland and Liptzin 2007), favor NH_4^+ uptake, while many phytoplankton taxa typically rely on NO_3^- (Redfield 1958), although nutrient preferences can vary by group and environmental conditions (Glibert et al. 2014). These functional and elemental differences likely underpinned the observed patterns of enzyme expression and biomass dynamics. Notably, the co-increase of both microbial groups before day 11, along with elevated enzyme activity associated with organic matter breakdown, points to a transient mutualistic interaction that shifted according to nutrient delivery mode.

Delivery mode alters biogeochemical trajectories

The frequency and concentration of nutrient inputs shaped not only biomass structure but also functional activity and biogeochemical conditions. While pulse treatments suggest accelerated microbial processing, continuous inputs maintained more stable DO and nutrient levels, supporting sustained microbial activity. Combined with the intermediate processes in the pulse–continuous treatments due to ongoing resource availability after the initial pulse, these findings support the idea that microbial communities respond not only to nutrient quantity but also to delivery mode, as has been observed in both Traving et al. (2017) and Butzler and Chase (2009). Furthermore, the ratio of bacterioplankton to phytoplankton biomass increased in the pulse and pulse–continuous treatments during the middle phase of the experiment (Fig. S3), suggesting a threshold response to nutrient concentration. While Tilman's Resource Supply Ratio Theory (Tilman 1982; Tilman et al. 1982) emphasized spatial resource heterogeneity, in aquatic systems temporal heterogeneity may be more influential (Yamamoto and Hatta 2004). If nutrient pulses occur at intervals mismatched with community recovery dynamics, they may drive functional shifts even under similar cumulative inputs (Nixon 1995; Smith et al. 1999).

Implications: "The lagoon quality paradox"

In the continuous nutrient treatments, inorganic nutrient concentrations remained low and comparable to the control. Yet, phytoplankton and bacterioplankton biomass, as well as extracellular enzyme activity (EEA), increased steadily over the 24-day experiment. These observations suggest that the system assimilated the continuous low-concentration inputs

rapidly enough that nutrient levels remained largely undetectable. Such dynamics reveal a system in which production proceeds under nutrient regimes that evade conventional detection, echoing the concept of the "Estuarine Quality Paradox" (Elliott and Quintino 2007).

Previous hydrological models and field studies have shown that subterranean groundwater can account for up to 80% of water inputs to Mediterranean lagoons, especially during summer months. This contribution is influenced by geomorphology and lithology (Meredith et al. 2022). Menció et al. (2023) noted nitrogen concentrations in surrounding groundwater can reach ~5 mg/L, making continuous low-level nutrient loading plausible. However, the rapid microbial uptake in these systems obscures this input, even as it sustains elevated production. These challenges are compounded by the high environmental variability in Mediterranean lagoons, where meteorological events strongly shape water chemistry and physical dynamics (Quintana et al. 2018). Such variability results in a low signal-to-noise ratio, making long-term nutrient trends difficult to detect and disentangle from natural fluctuations.

To overcome this paradox, Elliott and Quintino (2007) proposed developing methods that distinguish anthropogenic stress from natural variability. Our results support this, as a sustained, low-intensity nutrient influx exerted the strongest and most lasting bottom-up effect on plankton biomass and functional dynamics rather than high-concentration pulses. This implies that conventional monitoring based on nutrient thresholds may underestimate ecosystem alteration when nutrients are supplied in subtle, consistent ways.

To address these limitations, complementary tools are needed to capture the full spectrum of nutrient-driven impacts. A promising tool is the use of stable isotope techniques (e.g., $\delta^{15}N$ and $\delta^{13}C$) to trace nutrient sources and assimilation pathways. These methods can help identify groundwater-derived nitrogen and its incorporation into food webs, complementing functional indicators such as EEA and biomass. Their application in other Mediterranean lagoons, such as La Palme and Salses-Leucate (Andrisoa et al. 2019), shows their utility in revealing hidden nutrient dynamics. Further integration of nutrient stoichiometry, molecular markers, and multivariate analyses (including land use and hydrology) can enhance our ability to distinguish anthropogenic signals in naturally stressed systems (Savage et al. 2010; Borja et al. 2012). Without such approaches, diffuse inputs and the frequency of their availability may confound ecological assessments and lead to under-informed management.

Nevertheless, results here call for revisiting how ecological status is evaluated in coastal lagoons. The presence of a potential alternative stable state driven by nutrient assimilation uncoupled from measurable concentrations suggests that assessments based solely on detectable nutrients are insufficient. Delivery mode also needs to be considered when assessing eutrophication risk. Environmental policies must evolve to include temporal dynamics (e.g., stressor frequency and timing) and better account for low-level, chronic stressors (Sabater et al. 2019; Perujo et al. 2021). Doing so is critical for advancing effective ecosystem management and resilience in these vulnerable environments.

Supplementary Information The online version contains supplementary material available at https://doi.org/10.1007/s00027-026-01299-y.

Acknowledgements W.M. benefited from a Ph.D. grant (IFUdG 2019) from the University of Girona. This research is part of the CoMeDi—Respuesta a las perturbaciones a nivel de comunidad y metacomunidad en ecosistemas acuáticos someros (CGL2016-76024-R, AEI/FEDER/UE), Fun-metanet (PID2020-114440 GB-100), and AquiPondSys (PID2023-1471860B-100), grants, both funded by Spanish Ministry of Science and Innovation (MCIN)/AE/https://doi.org/10.13039/501100011033, and by "ERDF A way of making Europe" and conducted in the framework of European Union´s Horizon 2020 research and innovation program under grant agreement N° 869296 (The PONDERFUL Project). The manuscript was written by the authors, who take full responsibility for its content. An artificial intelligence (AI)-assisted language tool was used only for minor grammatical corrections and wording improvements.

Author contributions W.M.—conceptualization, methodology, investigation, formal analysis, visualization, and writing—original draft. N.P.—conceptualization, methodology, investigation, and writing—review and editing. M.A-P.—conceptualization, investigation, and writing—review and editing. A.R.— conceptualization, investigation, and writing—review and editing. D.B.— conceptualization, methodology, investigation, and writing—review and editing. J.C.—conceptualization, methodology, investigation, and writing—review and editing. M.B-S.—writing—review and editing. X.Q.—conceptualization, methodology, investigation, supervision, and writing—review and editing. A.M.—conceptualization, methodology, investigation, supervision, and writing—review and editing.

Funding Open Access funding provided by CERCA through the CRUE-CSIC agreement with Springer Nature. This work was supported by a Ph.D. grant (IFUdG 2019) from the University of Girona. This research is part of the CoMeDi—Respuesta a las perturbaciones a nivel de comunidad y metacomunidad en ecosistemas acuáticos someros (CGL2016-76024-R, AEI/FEDER/UE), Fun-metanet (PID2020-114440 GB-100) and AquiPondSys (PID2023-1471860B-100), grants, both funded by MCIN/AE/https://doi.org/10.13039/501100011033, and by "ERDF A way of making Europe" and conducted in the framework of European Union´s Horizon 2020 research and innovation program under grant agreement N° 869296 (The PONDERFUL Project).

Data availability The dataset on phytoplankton and bacterioplankton biomass, specific growth rate and nutrient uptake, as well as extracellular enzyme activity is available at https://doi.org/10.6084/m9.figshare.27909867. All other data are available on request.

Declarations

Conflict of interest The authors declare no competing interests.

References

Andrisoa A, Stieglitz TC, Rodellas V, Raimbault P (2019) Primary production in coastal lagoons supported by groundwater discharge and porewater fluxes inferred from nitrogen and carbon isotope signatures. Mar Chem 210:48–60. https://doi.org/10.1016/j.marchem.2019.03.003

Arnosti C (2011) Microbial extracellular enzymes and the marine carbon cycle. Annu Rev Mar Sci 3:401–425. https://doi.org/10.1146/annurev-marine-120709-142731

Atkins ML, Santos IR, Ruiz-Halpern S, Maher DT (2013) Carbon dioxide dynamics driven by groundwater discharge in a coastal floodplain creek. J Hydrol 493:30–42. https://doi.org/10.1016/j.jhydrol.2013.04.008

Badosa A, Boix D, Brucet S, López-Flores R, Quintana XD (2006) Nutrients and zooplankton composition and dynamics in relation to the hydrological pattern in a confined Mediterranean salt marsh (NE Iberian Peninsula). Estuar Coast Shelf Sci 66:513–522. https://doi.org/10.1016/j.ecss.2005.10.006

Bernhardt ES, Palmer MA (2011) The environmental costs of mountaintop mining valley fill operations for aquatic ecosystems of the Central Appalachians. Ann N Y Acad Sci 1223:39–57. https://doi.org/10.1111/j.1749-6632.2011.05986.x

Boadella J, Butturini A, Compte J, Gionchetta G, Perujo N, Quintana XD, Romaní AM (2021) Different microbial functioning in natural versus man-made Mediterranean coastal lagoons in relation to season. Estuar Coast Shelf Sci 259:107434. https://doi.org/10.1016/j.ecss.2021.107434

Borja Á, Elliott M, Andersen JH, Cardoso AC, Carstensen J (2012) Good environmental status of marine ecosystems: what is it and how do we know when we have attained it? Mar Pollut Bull 76(1–2):16–27. https://doi.org/10.1016/j.marpolbul.2012.09.001

Butzler JM, Chase JM (2009) The effects of variable nutrient additions on a pond mesocosm community. Hydrobiologia 617:65–73. https://doi.org/10.1007/s10750-008-9443-8

Cabrerizo MJ, Medina-Sánchez JM, Villar-Argaiz M, Carrillo P (2019) Interplay between resistance and resilience governs the stability of a freshwater microbial food web under multiple stressors. Sci Total Environ 660:1142–1150. https://doi.org/10.1016/j.scitotenv.2019.07.173

Carstensen J, Sánchez-Camacho M, Duarte CM, Krause-Jensen D, Marbà N (2011) Connecting the dots: responses of coastal ecosystems to changing nutrient concentrations. Environ Sci Technol 45(22):9122–9132. https://doi.org/10.1021/es202351y

Cleveland CC, Liptzin D (2007) C: N: P stoichiometry in soil: is there a "Redfield ratio" for the microbial biomass? Biogeochemistry 85(3):235–252. https://doi.org/10.1007/s10533-007-9132-0

Cloern JE (2001) Our evolving conceptual model of the coastal eutrophication problem. Mar Ecol Prog Ser 210:223–253

Cyronak T, Santos IR, Erler DV, Eyre BD (2013) Groundwater and porewater as major sources of alkalinity to a fringing coral reef lagoon (Muri Lagoon, Cook Islands). Biogeosciences 10:2467–2480. https://doi.org/10.5194/bg-10-2467-2013

De Vries W (2021) Impacts of nitrogen emissions on ecosystems and human health: a mini review. Curr Opin Environ Sci Health 21:100249. https://doi.org/10.1016/j.coesh.2021.100249

Elliott M, Quintino V (2007) The estuarine quality paradox, environmental homeostasis and the difficulty of detecting anthropogenic stress in naturally stressed areas. Mar Pollut Bull 54(6):640–645. https://doi.org/10.1016/j.marpolbul.2007.02.003

García-Robledo E, Revsbech NP, Corzo A (2016) Evidence of high nitrification rates in benthic biofilms of oligotrophic Mediterranean lagoons. Limnol Oceanogr 61(3):1039–1056. https://doi.org/10.1002/lno.10275

Gasol JM, Del Giorgio PA (2000) Using flow cytometry for counting natural planktonic bacteria and understanding the structure of planktonic bacterial communities. Sci Mar 64(2):197–224. https://doi.org/10.3989/scimar.2000.64n2, https://doi.org/10.3989/scimar.2000.64n2197

Glibert PM, Maranger R, Sobota DJ, Bouwman L (2014) The Haber Bosch–harmful algal bloom (HB–HAB) link. Environ Res Lett 9(10):105001. https://doi.org/10.1088/1748-9326/9/10/105001

Lindstrom MJ, Bates DM (1988) Newton–Raphson and EM algorithms for linear mixed-effects models for repeated-measures data. J Am Stat Assoc 83(404):1014–1022

Litchman E, Klausmeier CA (2008) Trait-based community ecology of phytoplankton. Annu Rev Ecol Evol Syst 39:615–639

Litchman E, Edwards KF, Klausmeier CA (2015) Microbial resource utilization traits and trade-offs: implications for community structure, functioning, and biogeochemical impacts at present and in the future. Front Microbiol 6:254. https://doi.org/10.3389/fmicb.2015.00254

López-Flores R, Boix D, Badosa A, Brucet S, Quintana XD (2006) Pigment composition and size distribution of phytoplankton in a confined Mediterranean salt marsh ecosystem. Mar Biol 149(6):1313–1324. https://doi.org/10.1007/s00227-006-0273-9

López-Flores R, Boix D, Badosa A, Brucet S, Quintana XD (2009) Environmental factors affecting bacterioplankton and phytoplankton dynamics in confined Mediterranean salt marshes (NE Spain). J Exp Mar Biol Ecol 369(2):118–126. https://doi.org/10.1016/j.jembe.2008.11.003

Lu C, Tian H (2017) Global nitrogen and phosphorus fertilizer use for agriculture production in the past half century: shifted hot spots and nutrient imbalance. Earth Syst Sci Data 9(1):181–192. https://doi.org/10.5194/essd-9-181-2017

McQueen DJ, Post JR, Mills EL (1986) Trophic relationships in freshwater pelagic ecosystems. Can J Fish Aquat Sci 43:1571–1581. https://doi.org/10.1139/f86-195

Menció A, Casamitjana X, Mas-Pla J, Coll N, Compte J, Martinoy M, Pascual J, Quintana XD (2017) Groundwater dependence of coastal lagoons: The case of La Pletera salt marshes (NE Catalonia). J Hydrol 552:793–806. https://doi.org/10.1016/j.jhydrol.2017.07.034

Menció A, Madaula E, Meredith W, Casamitjana X, Quintana XD (2023) Nitrogen in surface aquifer—coastal lagoons systems: analyzing the origin of eutrophication processes. Sci Total Environ 871:161947. https://doi.org/10.1016/j.scitotenv.2023.161947

Meredith W, Casamitjana X, Quintana XD, Menció A (2022) Effects of morphology and sediment permeability on coastal lagoons' hydrological patterns. J Hydrol 612:128259. https://doi.org/10.1016/j.jhydrol.2022.128259

Meredith W, Menció A, Antón-Pardo M, Romaní AM, Perujo N, Boix D, Gascón S, Compte J, Sala J, Bas-Silvestre M, Quintana XD (2025) Inorganic nutrient input effects and severity of disturbance in zooplankton community structure. Hydrobiologia. https://doi.org/10.1007/s10750-025-05998-9

Miller MB, Bassler BL (2001) Quorum sensing in bacteria. Annu Rev Microbiol 55:165–199. https://doi.org/10.1146/annurev.micro.55.1.165

Nixon SW (1995) Coastal marine eutrophication: a definition, social causes, and future concerns. Ophelia 41:199–219

Perujo N, Van den Brink PJ, Segner H, Mantyka-Pringle C, Sabater S, Birk S, Acuña V (2021) A guideline to frame stressor effects in freshwater ecosystems. Sci Total Environ 777:146112. https://doi.org/10.1016/j.scitotenv.2021.146112

Quintana XD, Antón-Pardo M, Bas-Silvestre M, Boix D, Casamitjana X, Compte J, Cunillera-Montcusí D, Gascón S, Menció A, Obrador B, Tornero I, Sala J (2021) Identifying critical transitions in seasonal shifts of zooplankton composition in a confined coastal salt marsh. Aquat Sci 83:69

Quintana XD, Boix D, Casamitjana X, Colomer A, Compte J, Cunillera-Montcusí D, Gascón S, Gich F, Menció A, Martinoy M, Montaner J, Pascual J, Sala J, Solà J, Tornero I (2018). Management and restoration actions of confined Mediterranean coastal lagoons in the Empordà and Baix Ter wetlands. In: Quintana, X.D.,

R Core Team (2021). R: a language and environment for statistical computing. R Foundation for Statistical Computing, Vienna, Austria.

Redfield AC (1958) The biological control of chemical factors in the environment. Am Sci 46(3):230A-A221

Romaní A, Artigas J, Ylla I (2012) Extracellular enzymes in aquatic biofilms: Microbial interactions vs water quality effects in the use of organic matter. In: Lear G, Lewis G (eds) Microbial biofilms: current research and applications. Caister Academic Press, pp 153–174

Sabater S, Elosegi A, Ludwig R (2019) Defining multiple stressor implications. In: Sabater S, Elosegi A, Ludwig R (eds) Multiple stressors in river ecosystems: status, impacts and prospects for the future. Elsevier Inc

Sarmento H, Gasol JM (2012) Use of phytoplankton-derived DOC by different types of bacterioplankton. Environ Microbiol 14(9):2348–2360. https://doi.org/10.1111/j.1462-2920.2012.02787.x

Savage C, Leavitt PR, Elmgren R (2010) Effects of land use on trophic status and ecosystem stability in a coastal bay. Limnol Oceanogr 55(3):1033–1045. https://doi.org/10.4319/lo.2010.55.3.1033

Smith VH, Tilman GD, Nekola JC (1999) Eutrophication: impacts of excess nutrient inputs on freshwater, marine, and terrestrial ecosystems. Environ Pollut 100:179–196. https://doi.org/10.1016/S0269-7491(99)00091-3

Sörenson E, Farnelid H, Lindehoff E, Legrand C (2020) Resource partitioning between phytoplankton and bacteria in the coastal Baltic Sea. Front Mar Sci 7:608244. https://doi.org/10.3389/fmars.2020.608244

Svensen C, Nejstgaard JC, Egge JK, Wassmann P (2002) Pulsing versus constant supply of nutrients (N, P and Si): effect on phytoplankton, mesozooplankton and vertical flux of biogenic matter. Sci Mar 66:189–203. https://doi.org/10.3989/scimar.2002.66n3189

Thingstad TF, Lignell R (1997) Theoretical models for the control of bacterial growth rate, abundance, diversity and carbon demand. Aquat Microb Ecol 13:19–27. https://doi.org/10.3354/ame013019

Tilman D (1982) Resource competition and community structure. Princeton University Press

Tilman D, Kilham SS, Kilham P (1982) Phytoplankton community ecology: the role of limiting nutrients. Annu Rev Ecol Syst 13:349–372. https://doi.org/10.1146/annurev.es.13.110182.002025

Traving SJ, Rowe O, Jakobsen NM, Sørensen SJ, Dittmar T, Stedmon CA (2017) The effect of increased loads of dissolved organic matter on estuarine microbial community composition and function. Front Microbiol 8:351. https://doi.org/10.3389/fmicb.2017.00351

Troussellier M, Courties C, Lebaron P, Servais P (1999) Flow cytometric discrimination of bacterial populations in seawater based on SYTO 13 staining of nucleic acids. FEMS Microbiol Ecol 29(4):319–330

Urvoy M, Labry C, L'Helguen S, Lami R (2022) Quorum sensing regulates bacterial processes that play a major role in marine biogeochemical cycles. Front Mar Sci. https://doi.org/10.3389/fmars.2022.834337

Vadstein O (2000) Heterotrophic, planktonic bacteria and cycling of phosphorus: phosphorus requirements, competitive ability and food web interactions. Adv Microb Ecol 16:115–168. https://doi.org/10.1007/978-1-4615-4187-5_4

Viaroli P, Bartoli M, Giordani G, Naldi M, Orfanidis S (2008) Community shifts, alternative stable states, biogeochemical controls and feedbacks in eutrophic coastal lagoons: a brief overview. Aquat Conserv 18(S1):S105–S117. https://doi.org/10.1002/aqc.956

Yamamoto T, Hatta G (2004) Pulsed nutrient supply as a factor inducing phytoplankton diversity. Ecol Model 171:247–270. https://doi.org/10.1016/j.ecolmodel.2003.08.011